HHS Public Access

Author manuscript

Nat Chem Biol. Author manuscript; available in PMC 2015 May 01.

Published in final edited form as:

Nat Chem Biol. 2014 November ; 10(11): 957–962. doi:10.1038/nchembio.1638.

Targeted Protein Destabilization Reveals an Estrogen-mediated ER Stress Response

Kanak Raina[1,*], **Devin J. Noblin**[2,*], **Yevgeniy V. Serebrenik**[2], **Alison Adams**[2], **Connie Zhao**[3], and **Craig M. Crews**[1,2,4]

[1]Department of Chemistry, Yale University, New Haven, Connecticut 06511, United States

[2]Department of Molecular, Cellular, and Developmental Biology, Yale University, New Haven, Connecticut 06511, United States

[3]Department of Molecular Biophysics and Biochemistry, Yale University, New Haven, Connecticut 06511, United States

[4]Department of Pharmacology, Yale University, New Haven, Connecticut 06511, United States

Abstract

Accumulation of unfolded proteins within the endoplasmic reticulum (ER) of eukaryotic cells leads to an unfolded protein response (UPR) that either restores homeostasis or commits the cells to apoptosis. Tools traditionally used to study the UPR are pro-apoptotic and thus confound analysis of long-term cellular responses to ER stress. Here, we describe an Endoplasmic Reticulum-localized HaloTag (ERHT) protein that can be conditionally destabilized using a small molecule hydrophobic tag (HyT36). Treatment of ERHT-expressing cells with HyT36 induces an acute, resolvable ER stress that results in transient UPR activation without induction of apoptosis. Transcriptome analysis of late-stage responses to this UPR stimulus reveals a link between UPR activity and estrogen signaling.

Introduction

Approximately one-third of all mammalian proteins are processed by the endoplasmic reticulum (ER)[1]. In order to handle this heavy workload, the ER contains high concentrations of proteins that facilitate protein folding and processing. When folding is unsuccessful, terminally misfolded proteins are retro-translocated to the cytosol, ubiquitylated, and degraded by the proteasome in a process called Endoplasmic Reticulum-Associated Degradation (ERAD)[2]. However, large accumulations of misfolded proteins can

*equal contributors

Competing Financial Interests: The authors declare no competing financial interests

Author Contributions

K.R. and D.J.N. contributed equally as first authors to this work. C.M.C conceived the idea. K.R. generated the ERHT construct and cell line, and performed the immunoprecipitation and immunoblotting studies. D.J.N., K.R., Y.V.S., and A.A. performed the qPCR experiments. D.J.N. analyzed the RNA-seq data. Y.V.S. and D.J.N. assessed compound cytotoxicity. C.Z. and Y.V.S. performed the ERAD experiments. D.J.N., K.R. and C.M.C. wrote the paper.

overwhelm the ERAD machinery and cause ER stress[3]. To sense and ameliorate ER stress, eukaryotic cells have evolved several mechanisms, which are collectively known as the Unfolded Protein Response (UPR). Low levels of stress are resolved via the adaptive mechanisms of the UPR; however, if the ER stress sensed by the cell cannot be remedied, pro-apoptotic UPR signaling becomes dominant, thereby eliminating cells unable to cope with disrupted protein folding in the ER.

The UPR in mammalian cells has traditionally been divided into three branches: IRE1, ATF6, and PERK, each named after an ER transmembrane protein that senses ER stress and initiates signaling events to restore homeostasis. The Inositol Requiring Enzyme 1 (IRE1) pathway is the only UPR branch conserved from yeast to mammals[4]. Although there are two IRE1 isoforms in mammals, the more widely distributed isoform is IRE1α[5]. Upon recognizing accumulated misfolded proteins in the ER lumen, IRE1α undergoes oligomerization[6] and autophosphorylation of its cytosolic kinase domain. This causes activation its RNase domain, which is responsible for an unconventional splicing event whereby mRNA transcripts encoding the X box-Binding Protein 1 (XBP1u) are processed to yield the basic Leu zipper (bZIP) transcription factor, XBP1s[7]. XBP1s induces the transcription of genes involved in functions such as protein folding, lipid biosynthesis, and ERAD[8]. In addition to XBP1 splicing, IRE1 also functions to selectively degrade mRNA that encode for ER-targeted proteins in order to reduce total protein load within the organelle[9]. This process, known as Regulated IRE1-Dependent Decay (RIDD), is also thought to play a role in non-specific degradation of ER localized mRNA during UPR-induced apoptosis[10,11].

Activating Transcription Factor 6 (ATF6) is an endoplasmic reticulum transmembrane protein that is translocated to the golgi under ER stress and is subsequently processed by site-1 and site-2 proteases to yield an N-terminal fragment[12]. This N-terminal fragment acts as a bZIP transcription factor that upregulates expression of several ER-resident proteins involved in homeostasis maintenance, such as the Hsp70-related chaperone BiP (GRP78/HSPA5). BiP binds to unfolded proteins in the ER, and it has been proposed that BiP binding to unfolded proteins may be an important step in the activation of IRE1α and ATF6[13].

Similarly to IRE1α, the Protein kinase R-like Endoplasmic Reticulum Kinase (PERK) is also activated via oligomerization and autophosphorylation[8]. Indeed, the luminal stress sensing domains of IRE1α and PERK are functionally interchangeable[14]. When activated, PERK phosphorylates and inactivates the Eukaryotic translation Initiator Factor 2α (eIF2α). This event, while attenuating global translation, favors the selective translation of a subset of mRNA, including activating transcription factor 4 (ATF4)[15]. ATF4 is a bZIP transcription factor that induces the expression of genes such as the transcription factor C/EBP Homologous Protein (CHOP) and Growth Arrest and DNA Damage-inducible 34 (GADD34). Whereas the attenuation of general translation via eIF2α phosphorylation promotes cell survival under ER stress[16], the induction of ATF4 and CHOP contributes to ATP depletion, oxidative stress, and eventual apoptosis[17].

ER stress in mammalian cells thus results in a seemingly paradoxical mixture of pro-survival and pro-apoptotic UPR signals. It has been proposed that the integration of these signals serves as a decision making process for cell fate[18], and some combination of intensity and duration of the stress plays a role in the outcome. Although some factors influencing the decision to switch between stress resolution and apoptosis have been elucidated, our understanding of the consequences of UPR signaling remains incomplete.

Tools that facilitate UPR activation have been essential in probing the molecular components involved in each pathway. These ER stressors can be broadly categorized into two classes: pharmacological tools and genetic tools.

Pharmacological tools typically activate the UPR by disrupting an endogenous pathway, leading to ER stress. For example, thapsigargin inhibits sarcoplasmic or endoplasmic reticulum Ca^{2+}-ATPase (SERCA) pumps, resulting in depletion of calcium reserves in the ER, a loss in activity of calcium-dependent chaperones, and subsequent protein misfolding within the ER[19]. The natural product tunicamycin inhibits N-linked glycosylation, thus producing incompletely processed proteins within the ER[20]. Brefeldin A inhibits nucleotide exchange on the ARF-1 protein necessary for golgi trafficking, which results in a rapid accumulation of normally-trafficked proteins within the ER[21]. All of these traditional ER stressors are toxic compounds that induce apoptosis, which can limit their utility in studying UPR signaling. Specifically, pharmacological stressors that cause global unfolding of ER resident proteins have the potential to impact any signaling events that involve said proteins and may thereby confound UPR signaling analysis. Additionally, the very tight binding of agents such as thapsigargin makes inhibition practically irreversible, persisting after dilution or removal of excess inhibitor[19]. Similarly, even a short pulse with tunicamycin has apoptotic activity in some cellular contexts[22].

For the reasons listed above, attempts have been made to study the UPR by inducing the overexpression of an ectopic, misfolded protein within the ER[23]. However, these methods typically cannot activate the UPR with the same strength and kinetics as pharmacological agents. In some cases, misfolded proteins induce no activation of one or more of the UPR pathways[24–27]. Similarly, the Destabilizing Domain (DD) dependent small molecule driven protein degradation system also fails to cause a sufficient insult upon withdrawal of the Shield-1 stabilizing ligand to induce UPR activation[28]. Taken together, these reports suggest that simply overexpressing a single misfolded protein in the ER is inadequate to provide a robust UPR response with temporal control over activity.

Recently, independent control over protein levels of XBP1s and ATF6 in the same cell using two orthogonal small molecules was described[1]. This system significantly improved the understanding in the field regarding the influence of these two transcription factors on the UPR transcriptome, and it complements another recent report that focuses on the transcriptional effects of the PERK pathway via ATF4 and CHOP[17].

The tools described above have inherent limitations in terms of intensity of stress, temporal control, physiological relevance, and stress resolvability. An aspect of ER biology that remains unexplored, therefore, is the nature of the cellular response to an acute stress that

can be resolved and does not lead to apoptosis. We reasoned that a tool engineered to explore this point may reveal new facets of UPR signaling that are observable only during later stages of the adaptive process and are typically masked by the apoptotic or non-specific effects of traditional ER stressors.

We recently described a system whereby small molecule hydrophobic tag (HyT) compounds can induce the thermodynamic destabilization of the HaloTag protein[29–31]. When expressed in the cytosol, this destabilized protein is recognized by chaperones including Hsp70 and is targeted for degradation by the ubiquitin-proteasome system. In the following study, we demonstrated that HyT-induced destabilization of a version of the HaloTag protein localized to the ER robustly activates the UPR. We also showed that, in contrast to the pharmacological stressors like tunicamycin and thapsigargin, the UPR induced by our system is transient and non-apoptotic. Finally, we used this HyT-Halotag system to analyze late-term transcriptomic effects of the UPR and discovered that induction of ER stress results in an upregulation of estrogen signaling.

Results

Localization of HaloTag to the Endoplasmic Reticulum

To create the Endoplasmic Reticulum-localized HaloTag (ERHT) construct, we fused HaloTag to EGFP along with the Calreticulin N-terminal signal sequence as well as the C-terminal ER retention sequence, KDEL[32,33] (Fig. 1a). We then stably integrated this construct into HEK293 cells using the Flp-In recombination system. The ERHT protein did indeed localize to the ER, as confirmed by confocal microscopy and co-staining with an endoplasmic reticulum selective dye (Fig. 1b). The ERHT protein and the ER-ID stain yielded Manders' Colocalization Coefficients[34] of M1 = 0.94 and M2 = 0.93, respectively (Supplementary Results, Supplementary Fig. 1). Based on its exquisite ability to induce the misfolding and degradation of the cytosolic version of the HaloTag protein, we chose the hydrophobic tag HyT36[30] (Fig. 1c) for this study.

Destabilization of the ERHT protein using HyT36

We first tested whether HyT36 had the desired effect of destabilizing the ERHT protein. To determine this, we examined ERHT protein solubility after binding to HyT36. We lysed ERHT-expressing cells, and treated the lysate with either HyT36 (10 μM) or DMSO (0.1%) and incubated the solution at 37 °C for 1 hour. We then centrifuged the solutions at 16,000 g for 20 minutes to generate a pellet fraction, washed the pellet, and then quantified ERHT levels in the pellet by Western blotting. We found that HyT36-treatment increased the amount of ERHT protein in the insoluble pellet fraction, suggesting a HyT36-induced reduction in ERHT protein stability (Fig. 2a, see Supplementary Fig. 2 for quantification).

Next, we tested whether treatment of ERHT-expressing cells with HyT36 induced unfolding of the protein in the cellular context. Indeed, HyT36 addition to cells induced association of the ERHT protein with IRE1α[35] and with BiP/GRP78 at both the 1h and 4h time points (Fig. 2b, see Supplementary Fig. 3 for quantification). Blocking new protein synthesis with

cycloheximide did not affect the induction of BiP binding upon HyT36 treatment, supporting a post-translational effect (Supplementary Fig. 4).

UPR activation in ERHT-expressing Cells

Having verified that HyT36 treatment can destabilize the ERHT protein in cells, we examined whether HyT36 treatment in these cells would activate the unfolded protein response (UPR). We compared UPR activation observed after HyT36 treatment to UPR activation observed using two traditional ER stressors, thapsigargin and tunicamycin. We first measured activation of two UPR branches via Western blot: 1) phosphorylation of eukaryotic translation initiation factor 2α (EIF2α) as a readout of PERK activity, and 2) expression of X-box-binding protein 1 splicing variant (XBP1s) as a readout of IRE1α activity (Fig. 3a). Both pathways were activated to similar extents with 10 μM HyT36 and 500nM thapsigargin, whereas 5 μg/mL tunicamycin yielded a smaller response.

To further test activation of the ATF6 and IRE1α pathways, we stably integrated luciferase reporters into ERHT-expressing cells. We used the section of XBP1 mRNA containing the Ire1 target intron to construct a reporter for this pathway, whereby splicing by the IRE1α RNase causes a frameshift that results in expression of the NanoLuc luciferase protein. In the case of the previously characterized unfolded protein response element (UPRE) reporter[36], upregulation of ATF6 or Xbp1s transcriptional activity results in expression of the firefly luciferase protein. Use of these luciferase reporters confirmed that HyT36 treatment activated the UPR to similar extents as the traditional ER stressors, thapsigargin and tunicamycin (Fig. 3b).

As a final confirmation that all three UPR pathways were activated in ERHT cells by HyT36 treatment, we performed qPCR analysis on a panel of genes regulated by IRE1α[1], ATF6[1], and PERK[17] (Fig. 3c). HyT36 treatment gave similar levels of UPR activation as tunicamycin in all cases except, interestingly, the transcriptional regulation of CHOP and TRIB3, both of which were significantly more responsive to tunicamycin. Additionally, we evaluated IRE1α RNase activity by looking directly at XBP1 mRNA splicing (Supplementary Fig. 5). Also, we determined the dependence of select UPR target gene levels on the concentration of HyT36, and compared this response to that elicited by tunicamycin and thapsigargin (Supplementary Fig. 6). We observed that as little as 500nM HyT36 was sufficient to produce a robust UPR response. It is important to mention that we chose a maximum concentration of 10μM HyT36 in this experiment because a higher concentration of 30 μM appeared to affect cell viability even in parental FlpIn cells lacking the ERHT construct (Supplementary Fig. 7).

To confirm that modulation of the thermodynamic stability of the ERHT protein was sufficient to cause a marked effect of the kind HyT36 treatment had on the UPR, we treated ERHT cells with a HaloTag stabilizer molecule (HALTS1), which binds to HaloTag and functions as a pharmacological chaperone, resulting in an increase in its thermodynamic stability[29]. HALTS1 treatment lowered the basal levels of UPR-induced genes such as ERDJ4, HYOU1, and BiP (Supplementary Fig. 8). These data lend support to the idea that increasing or decreasing the thermodynamic stability of this single ectopic protein can increase or decrease ER stress.

We next confirmed that the observed UPR activation with HyT36 was dependent upon the presence of the ERHT protein in the cells and not due to some off-target effect of the small molecule. We treated both the ERHT-expressing cells and the "parental" HEK293 cells, which do not express any ectopic protein, with HyT36 or thapsigargin and measured the activation of IRE1α via Xbp1s Western blot (Supplementary Fig. 9a). As expected, we observed no induction of XBP1s levels in the parental cells. Interestingly, thapsigargin appeared to induce XBP1 splicing to a lesser extent in the ERHT cells than in parental cells. We also confirmed that none of the UPR pathways were activated by HyT36 in parental cells by quantitative real-time PCR of their target genes (Supplementary Fig. 9b). Here too, 10μM HyT36 treatment showed no induction of any of the genes tested, in contrast to thapsigargin, which caused a robust induction in all of their levels.

HyT36 Transiently Activates UPR without Inducing Apoptosis

To determine whether HyT36 induced UPR activity was sustained or transient, we performed quantitative real-time PCR analysis to evaluate the effect of HyT36 on several UPR target genes (ERDJ4, BiP, CHOP) at a later 10 hour time point: In all three cases, treatment with HyT36 for two hours gave similar levels of UPR activation as traditional ER stressors, thapsigargin and tunicamycin. However, at the later ten-hour time point, UPR activity induced by HyT36 had returned to basal levels (Fig. 4a). In contrast, activity was still measurable in all three pathways after treatment with thapsigargin and tunicamycin. Furthermore, CHOP mRNA levels, a hallmark of UPR-induced apoptosis, were still increasing with both of these molecules.

We confirmed that the resolution of HyT36-induced ER stress was not due to degradation of the compound during prolonged treatment (Supplementary Fig. 10a) and that supplementing media with fresh HyT36 at intermediate time-points did not confer additional UPR activation (Supplementary Figs. 10b, 10c). Approximately 25% of the ERHT protein had been degraded by ERAD machinery by the later 10 hour time point (Fig. 4b, 4c). However, the ERHT protein remained destabilized, as measured by increased BiP binding, even at the 10 hour time point when UPR activity had been mostly resolved (Fig. 4d). Notably, we were not able to achieve transient UPR activation with thapsigargin even under pulsatile treatment conditions (Supplementary Fig. 11).

Mirroring CHOP kinetics, the transcription factor responsible for CHOP expression, ATF4, was also still increasing at the 10-hour time point after thapsigargin or tunicamycin treatment but not after HyT36 treatment (Fig. 5a). This led us to examine apoptosis. Strikingly, thapsigargin and tunicamycin treatment did indeed induce apoptosis after 24 hours of treatment, whereas HyT36 treatment did not, as determined by PARP cleavage (Fig. 5b), direct cell counting (Fig. 5c), and an MTS viability assay (Supplementary Fig. 12).

Estrogen Signaling Upregulation in Response to ER Stress

We used mRNA-seq to examine changes in gene expression in ERHT-expressing cells after 2-hour and 10-hour treatments with DMSO (0.1%), HyT36 (10 μM), thapsigargin (500 nM), or tunicamycin (5 μg/mL). After confirming that our mRNA-seq samples exhibited the expected UPR responses (Supplementary Table 1), we used Ingenuity Pathway Analysis to

help analyze the gene count data provided by the Genome Technology Access Center at Washington University, St. Louis (Supplementary Data Set 1). The ESR1 gene, encoding estrogen receptor (ERα), was listed as a master regulator of gene networks identified in the HyT36 10 hour time point (p value = 0.0015). We confirmed by qPCR the increased expression of 8 genes that were upregulated in our RNAseq sample and identified by Ingenuity Pathway Analysis to be downstream of the estrogen receptor: CRABP2[37], IFI27[38], SLC6A9[39], PDK2[40], SULF1[41], HOXD4[42], EGF[43], and SLC13A4[41] (Fig. 6a). Validation with qPCR confirmed that these genes were not upregulated upon HyT36 treatment in parental FlpIn HEK293 cells, which do not express the ERHT construct (Supplementary Fig. 13).

We next tested whether estrogen signaling as a consequence of the UPR could be observed even with traditional ER stressors in MCF7 cells which, in contrast to 293s, express high levels of Estrogen Receptors. Using an Estrogen Response Element (ERE) luciferase reporter, we observed that UPR activation with thapsigargin or tunicamycin also induces estrogen signaling, albeit to a significantly lesser extent than estradiol treatment (Fig. 6b). Incubation with the IRE1α RNase inhibitor 4μ8c inhibited reporter activation by thapsigargin but not by estradiol (Supplementary Fig. 14).

Discussion

Pharmacological tools currently used to study ER stress are pro-apoptotic small molecules that cause global protein unfolding within the endoplasmic reticulum, and thus have the potential to impact all cellular signaling that involves proteins passing through the secretory pathway. On the other hand, attempts to induce stress with ER-localized ectopically expressed unfolded proteins have yielded inconsistent results lacking in robustness of the UPR response and in temporal control over its induction.

The ERHT/HyT36 system described here is based on the premise that the unfolding of a single protein within the ER with a small molecule is a significantly improved tool to study ER stress, combining the advantages of temporal control provided by conventional stressors like tunicamycin and thapsigargin, and the specificity of ectopically expressed misfolded proteins. We had previously shown that the hydrophobic tag HyT36 can bind to the HaloTag protein *in vitro* and lower its thermodynamic stability, as measured by a decrease in protein melting temperature[30]. Therefore, we predicted that binding of HyT36 to ER-localized HaloTag (ERHT) would cause it to unfold and induce the UPR (Supplementary Fig. 15). We found that this was indeed the case, and that the HyT36 induced UPR was robust, operating through the expected mechanism whereby the unfolded protein was recognized by the elements of the ER quality control machinery. Interestingly, we were able to show that a pharmacological chaperone that binds and stabilizes the HaloTag protein (HALTS1) can lower the constitutive level of UPR signaling active in ERHT cells. This observation lends further support to our hypothesis that it is the modulation of the thermodynamic stability of the ERHT protein that is responsible for the marked effects on UPR signaling observed with our system.

Since the ERHT/HyT36 system induces ER stress through unfolding of a single protein, we asked whether the cell could resolve or adapt to this stress and avoid committing to apoptosis. When we analyzed the expression of a number of UPR target genes at both mRNA and protein level, we discovered that, in contrast to tunicamycin and thapsigargin, the ER stress induced by HyT36 was short-lived, and by 10 hours after HyT36 addition to cells, UPR target genes had returned to basal levels. We hypothesized that the resolvability of the HyT36-induced ER stress might partially be explained by ERHT protein degradation. Indeed, we found that ERHT protein levels were lowered via ERAD by about 25% over 10 hours with HyT36 treatment. Interestingly, we saw no drop-off in levels of ERHT mRNA over the same time course. We found that resolution of HyT36-induced UPR occurs even though a proportion of the ERHT protein remains misfolded and undegraded even at the 10 hour time point of HyT36 addition, as measured by levels of bound BiP. Based on these results, we hypothesize that a combination of ERHT protein degradation by ERAD and the induction of the adaptive UPR is responsible for the resolution of HyT36 induced UPR. Given this resolution, we were not surprised to find that unlike thapsigargin and tunicamycin, HyT36 was non-toxic to cells. We observed no PARP cleavage and no loss in cell number after a 24 hour HyT36 treatment.

The ERHT/HyT36 system thus provides a unique opportunity to study the effects of an acute ER stress that can be resolved by the cell. Unlike traditional ER stressors, such as thapsigargin and tunicamycin, targeted destabilization of the ERHT protein induces ER stress that can be resolved and does not induce apoptosis. Unlike systems inducing the expression of a constitutively misfolded protein, the targeted destabilization of the ERHT protein allows simultaneous unfolding of the target protein population on command. This leads to two significant advantages: UPR activation is as rapid and intense as traditional ER stressors, and the ER stress can be resolved within several hours without inducing apoptosis. Therefore, we hypothesized that this system may allow us to examine changes in the cell during late-stage stress resolution or after the resolution process. In other words, what genes are upregulated during late time points of UPR activation that might have a role in adapting the cell to ER stress? It should be noted that some cellular events during the later period would be masked in an experiment using traditional ER stressors due to significant apoptotic signaling. Additionally, transcriptionally inducible misfolded proteins do not provide the same temporal control over UPR activation.

We identified ESR1 signaling as being upregulated in a 10 hour treatment with HyT36 and not with thapsigargin or tunicamycin, even though several estrogen signaling genes in our list were upregulated by a 10 hour treatment with these compounds (Supplementary Table 2). Given the limited activation of ESR1 genes by HyT36 in ERHT cells, we reasoned that thapsigargin and tunicamycin may also induce estrogen signaling through their activation of the UPR, but the effect may have been masked by apoptotic or non-UPR signaling in those samples. This may in part be due to the low abundance of estrogen receptor in our ERHT cells, which yielded gene counts for ESR1 of approximately 5 counts per million. Indeed, we found that in MCF7 cells, which express high levels of Estrogen Receptors, we could induce estrogen signaling with thapsigargin and tunicamycin. Based on a previous report that XBP1s can interact with Estrogen Receptor binding sites and promote Estrogen Receptor transcriptional activity[44], we hypothesized that the Estrogen Receptor activity

induced by ER stress might be proceeding through IRE1α-dependent generation of XBP1s. In support of this reasoning, we found that pretreatment of MCF7 cells with the Ire1α inhibitor 4μ8c attenuated thapsigargin induced ERE-luciferase activity.

Although we decided to use the ERHT/HyT36 system to study gene expression profiles in the cell after an acute ER stress, we believe this system could be used in a number of ways to study the UPR. For example, it would be interesting to characterize the contribution of different mechanisms such as increased chaperone and foldase expression, increased ER volume, and increased ERAD activity. Similarly, it would be interesting to understand whether any changes to the ER persist long after the stress has been resolved. The ERHT/HyT36 system may prove to be a useful tool to study many aspects of ER regulation that cannot be studied using the tools currently available. Lastly, it would be interesting to test if the ERHT/HyT36 system could be expanded to study the mitochondrial UPR. This would simply involve placing a mitochondrial localization signal on the HaloTag protein and studying its unfolding upon HyT36 treatment. mtUPR is currently studied with the help of inducers such as overexpressed misfolded proteins[45,46] or mitochondria-targeted pro-apoptotic Hsp90 inhibitors such as Gamitrinibs[47,48]. Future work using this system may yield a complementary small molecule based tool to study the mtUPR.

Online Methods

Cell culture

HEK293 cells used in this study were FRT recombination-based 293 Flp-In cells (Invitrogen), which were cultured in Dulbecco's Modified Eagle Medium (DMEM) from Life Technologies. MCF7cells were cultured in Gibco® RPMI1640 medium. All growth media were supplemented with 10% Fetal Bovine Serum (FBS, Gibco®), 100 U mL^{-1} penicillin and 100 μg mL^{-1} streptomycin (Gibco®). For experiments involving β-estradiol treatment, at least one day prior to the experiment, cells were incubated in phenol red-free RPMI 1640 (Gibco®) containing 10% charcoal/dextran-treated FBS (HyClone).

Reagents

Monoclonal Antibodies against pEIF2α (#3398), Eif2α (#5324), IRE1α (#3294), PERK (#3192), BiP (#3177), and HA (#3724) were purchased from Cell Signaling. The anti-XBP1s monoclonal was purchased from Biolegend (#647502). ATF4 and ATF6 antibodies were supplied by SantaCruz Biotech (sc-200) and Abcam (ab122897) respectively. HyT36 was synthesized in the Crews lab and has been characterized previously.[30] Epoxomicin was synthesized in the Crews lab and has been characterized previously.[49] Tunicamycin, thapsigargin, and β-estradiol were purchased from Sigma Aldrich. The IRE1a RNase inhibitor 4μ8c was purchased from Calbiochem.

The ERHT plasmid was constructed using the pcDNA5/FRT vector (Life Technologies). The HaloTag2 template has been described previously[31]. We included the 17 amino-acid signal sequence from Calreticulin followed by EGFP at the N-terminus of HaloTag2, and the KDEL ER-retention signal at the C-terminus. The XBP1-Luciferase reporter was constructed with a 3-way USER Friendly Cloning Reaction using the pcDNA3 vector (Life Technologies), destabilized NanoLuciferase (NLucP) from Promega (Madison, WI) and an

XBP1-GFP reporter plasmid that was a gift from Prof. Maho Niwa (UCSD). The UPRE-driven firefly luciferase reporter plasmid, p5xATF6-GL3, was purchased from Addgene. The estrogen response element-driven firefly luciferase reporter plasmid, 3xERE TATA Luc, was purchased from Addgene.

Immunoprecipitation and immunoblotting

Cells were grown in 10cm plates, and treated with DMSO, HyT36, thapsigargin, or tunicamycin for indicated times. For western analysis of endoplasmic reticulum stress pathways, cells were lysed in a high salt RIPA buffer (40mM Tris pH 7.5, 500mM NaCl, 1% NP-40, 0.1% SDS, 0.5% sodium deoxycholate) supplemented with protease and phosphatase inhibitors, and sonicated briefly. Protein concentrations were normalized using a BCA assay, and 20–60ug total protein per sample were loaded on an SDS-PAGE gel. Further processing followed standard protocols. To detect binding of the HaloTag protein to endoplasmic reticulum stress receptors, cells were lysed in a buffer containing 40mM Tris pH 7.5, 150mM NaCl, 1% Tx-100, and protease inhibitors. Protein concentrations were normalized with a BCA assay and 1mg of total protein per sample was incubated for 2h with EZview Red Anti-HA affinity gel (Sigma) that had previously been blocked with 3% BSA in lysis buffer. The beads were subsequently centrifuged and washed three times with lysis buffer and suspended and boiled in 2x Laemmli buffer. Samples were loaded on an SDS-PAGE gel and western blotting was done following standard protocols.

Repeated HyT36 Treatments

ERHT cells in a 6-well plate were treated with 2mL of DMEM containing DMSO (0.1%) or HyT36 (10 μM). To one set, 1mL of DMSO (0.1%) or HyT36 (10 μM) was added every 2.5h, for a total of 4 treatments and a final volume of 5mL. All Cells were collected after 10 hours of treatment and processed for immunoblotting.

Thapsigargin Pulse Treatment

ERHT cells were treated with DMSO (0.1%), thapsigargin (500 nM), or HyT36 (10 uM) under two conditions: Under standard conditions (10 h treatment), cells were treated for 10 consecutive hours before assessing pro-apoptotic UPR signaling with a Western blot for ATF4. Under washout conditions (2h treatment + 8 h washout), cells were incubated with the indicated treatment for 2 hours, were then washed with PBS, and were then incubated in standard growth media for 8 hours before assessing ATF4 protein levels.

Confocal microscopy

ERHT cells were seeded at approximately 40% confluency on cover slips pre-coated with Cell-Tak (BD). The next day, cells were fixed and stained for endoplasmic reticulum with the ER-ID Red assay kit (Enzo Life Sciences) using the provided protocol. Cells were then mounted on Superfrost Plus microscope slides (Thermo Scientific) with Vectashield mounting medium (Vector Laboratories). Images were acquired using a Zeiss LSM 510 confocal microscope (Zeiss). Manders' colocalization coefficients were calculated using ImageJ software.

Luciferase reporter assays

Cells were resuspended in the growth medium at 100,000 cells/mL. 25 μL of media was then added to each well in a white, 384-well tissue culture-treated plate (Corning). For the XBP1s luciferase reporter, the plate was assayed using NanoGLO (Promega) following manufacturer's instructions. For the UPRE reporter, firefly luciferase activity was measured after treatment.

Real-time quantitative PCR

Total RNA was isolated using the RNeasy Mini Kit (Qiagen). cDNA was then created using the High Capacity cDNA Reverse Transcription Kit (Applied Biosystems). Real time quantitative PCR was then performed using FastStart Universal SYBR Green Master [ROX] (Roche) on a CFX96 Real-Time System (Bio-Rad). For primer sequences, see Supplementary Table 3.

XBP1 visualization by PCR

cDNA was generated from treated cells as described above. PCR reactions were carried out (primers XBP1F: GAGTTAAGACAGCGCTTGGG and XBP1R: ACTGGGTCCAAGTTGTCCAG) using GoTaq from Promega. The reaction was then digested with PstI, which cleaves the unspliced XBP1 amplicon to yield the 2u and 3u fragments, and run on a 3% agarose gel.

mRNA sequencing

Sample preparation, sequencing, and gene calling were performed by the Genome Technology Access Center at Washington University in St. Louis as described on their website.

Toxicity assays

For the MTS readout, cells were resuspended in the appropriate media at 400,000 cells per mL, and 50 μL were added per well to a 96 well tissue culture-treated plate (Corning). Cells were then treated with 50 μL of 2x media with the corresponding compounds and incubated for 24 hours. MTS conversion was then measured using the CellTiter 96 AQueous Non-Radioactive Cell Proliferation Assay (Promega). For the cell counting experiments, cells were treated in 6-well plates. 24h later, they were trypsinized and resuspended in 1mL of growth medium. Cell counting was done using a BioRad TC20 automated cell counter in biological and technical triplicates.

Graphing and Statistical Analysis

P-values for network enrichment in the RNA-sequencing data were provided by Ingenuity Pathway Analysis (IPA) as described[50]. Graphs were generated and t-tests were performed in GraphPad Prism.

Supplementary Material

Refer to Web version on PubMed Central for supplementary material.

Acknowledgments

We wish to acknowledge financial support from the US NIH (R01AI084140, R01CA083049) and the Department of Defense (DoD) through the National Defense Science & Engineering Graduate Fellowship (NDSEG) Program.

References

1. Shoulders MD, et al. Stress-independent activation of XBP1s and/or ATF6 reveals three functionally diverse ER proteostasis environments. Cell Rep. 2013; 3:1279–92. [PubMed: 23583182]
2. Smith MH, Ploegh HL, Weissman JS. Road to ruin: targeting proteins for degradation in the endoplasmic reticulum. Science. 2011; 334:1086–90. [PubMed: 22116878]
3. Bernasconi R, Galli C, Kokame K, Molinari M. Autoadaptive ER-Associated Degradation Defines a Preemptive Unfolded Protein Response Pathway. Mol Cell. 2013; 52:783–93. [PubMed: 24239290]
4. Mori K. Signalling pathways in the unfolded protein response: development from yeast to mammals. J Biochem. 2009; 146:743–50. [PubMed: 19861400]
5. Tirasophon W, Welihinda AA, Kaufman RJ. A stress response pathway from the endoplasmic reticulum to the nucleus requires a novel bifunctional protein kinase/endoribonuclease (Ire1p) in mammalian cells. Genes Dev. 1998; 12:1812–24. [PubMed: 9637683]
6. Korennykh AV, et al. The unfolded protein response signals through high-order assembly of Ire1. Nature. 2009; 457:687–93. [PubMed: 19079236]
7. Calfon M, et al. IRE1 couples endoplasmic reticulum load to secretory capacity by processing the XBP-1 mRNA. Nature. 2002; 415:92–6. [PubMed: 11780124]
8. Walter P, Ron D. The unfolded protein response: from stress pathway to homeostatic regulation. Science. 2011; 334:1081–6. [PubMed: 22116877]
9. Coelho DS, et al. Xbp1-independent Ire1 signaling is required for photoreceptor differentiation and rhabdomere morphogenesis in Drosophila. Cell Rep. 2013; 5:791–801. [PubMed: 24183663]
10. Han D, et al. IRE1alpha kinase activation modes control alternate endoribonuclease outputs to determine divergent cell fates. Cell. 2009; 138:562–75. [PubMed: 19665977]
11. Tabas I, Ron D. Integrating the mechanisms of apoptosis induced by endoplasmic reticulum stress. Nat Cell Biol. 2011; 13:184–90. [PubMed: 21364565]
12. Haze K, Yoshida H, Yanagi H, Yura T, Mori K. Mammalian transcription factor ATF6 is synthesized as a transmembrane protein and activated by proteolysis in response to endoplasmic reticulum stress. Mol Biol Cell. 1999; 10:3787–99. [PubMed: 10564271]
13. Bertolotti A, Zhang Y, Hendershot LM, Harding HP, Ron D. Dynamic interaction of BiP and ER stress transducers in the unfolded-protein response. Nat Cell Biol. 2000; 2:326–32. [PubMed: 10854322]
14. Liu CY, Schroder M, Kaufman RJ. Ligand-independent dimerization activates the stress response kinases IRE1 and PERK in the lumen of the endoplasmic reticulum. J Biol Chem. 2000; 275:24881–5. [PubMed: 10835430]
15. Harding HP, et al. Regulated translation initiation controls stress-induced gene expression in mammalian cells. Mol Cell. 2000; 6:1099–108. [PubMed: 11106749]
16. Harding HP, Zhang Y, Bertolotti A, Zeng H, Ron D. Perk is essential for translational regulation and cell survival during the unfolded protein response. Mol Cell. 2000; 5 :897–904. [PubMed: 10882126]
17. Han J, et al. ER-stress-induced transcriptional regulation increases protein synthesis leading to cell death. Nat Cell Biol. 2013; 15:481–90. [PubMed: 23624402]
18. Hetz C. The unfolded protein response: controlling cell fate decisions under ER stress and beyond. Nat Rev Mol Cell Biol. 2012; 13:89–102. [PubMed: 22251901]
19. Lytton J, Westlin M, Hanley MR. Thapsigargin inhibits the sarcoplasmic or endoplasmic reticulum Ca-ATPase family of calcium pumps. J Biol Chem. 1991; 266:17067–71. [PubMed: 1832668]
20. Takatsuki A, Arima K, Tamura G. Tunicamycin, a new antibiotic. I. Isolation and characterization of tunicamycin. J Antibiot (Tokyo). 1971; 24:215–23. [PubMed: 5572750]

21. Helms JB, Rothman JE. Inhibition by brefeldin A of a Golgi membrane enzyme that catalyses exchange of guanine nucleotide bound to ARF. Nature. 1992; 360:352–4. [PubMed: 1448152]
22. Carlberg M, et al. Short exposures to tunicamycin induce apoptosis in SV40-transformed but not in normal human fibroblasts. Carcinogenesis. 1996; 17:2589–96. [PubMed: 9006093]
23. Kaufman RJ. Stress signaling from the lumen of the endoplasmic reticulum: coordination of gene transcriptional and translational controls. Genes Dev. 1999; 13:1211–33. [PubMed: 10346810]
24. Lawless MW, et al. Activation of endoplasmic reticulum-specific stress responses associated with the conformational disease Z alpha 1-antitrypsin deficiency. J Immunol. 2004; 172:5722–6. [PubMed: 15100318]
25. Hidvegi T, Schmidt BZ, Hale P, Perlmutter DH. Accumulation of mutant alpha1-antitrypsin Z in the endoplasmic reticulum activates caspases-4 and -12, NFkappaB, and BAP31 but not the unfolded protein response. J Biol Chem. 2005; 280:39002–15. [PubMed: 16183649]
26. Mori A, et al. Derlin-1 overexpression ameliorates mutant SOD1-induced endoplasmic reticulum stress by reducing mutant SOD1 accumulation. Neurochem Int. 2011; 58:344–53. [PubMed: 21185345]
27. Nadanaka S, Yoshida H, Kano F, Murata M, Mori K. Activation of mammalian unfolded protein response is compatible with the quality control system operating in the endoplasmic reticulum. Mol Biol Cell. 2004; 15:2537–48. [PubMed: 15020717]
28. Sellmyer MA, Chen LC, Egeler EL, Rakhit R, Wandless TJ. Intracellular context affects levels of a chemically dependent destabilizing domain. PLoS One. 2012; 7:e43297. [PubMed: 22984418]
29. Neklesa TK, et al. A bidirectional system for the dynamic small molecule control of intracellular fusion proteins. ACS Chem Biol. 2013; 8:2293–300. [PubMed: 23978068]
30. Tae HS, et al. Identification of hydrophobic tags for the degradation of stabilized proteins. Chembiochem. 2012; 13:538–41. [PubMed: 22271667]
31. Neklesa TK, et al. Small-molecule hydrophobic tagging-induced degradation of HaloTag fusion proteins. Nat Chem Biol. 2011; 7:538–43. [PubMed: 21725302]
32. Munro S, Pelham HR. A C-terminal signal prevents secretion of luminal ER proteins. Cell. 1987; 48:899–907. [PubMed: 3545499]
33. Pelham HR. Evidence that luminal ER proteins are sorted from secreted proteins in a post-ER compartment. EMBO J. 1988; 7:913–8. [PubMed: 3402439]
34. Manders E. Measurement of colocalization of objects in dual-color confocal images. J Microsc. 1993; 169:8.
35. Gardner BM, Walter P. Unfolded proteins are Ire1-activating ligands that directly induce the unfolded protein response. Science. 2011; 333:1891–4. [PubMed: 21852455]
36. Wang Y, et al. Activation of ATF6 and an ATF6 DNA binding site by the endoplasmic reticulum stress response. J Biol Chem. 2000; 275:27013–20. [PubMed: 10856300]
37. Lu M, Mira-y-Lopez R, Nakajo S, Nakaya K, Jing Y. Expression of estrogen receptor alpha, retinoic acid receptor alpha and cellular retinoic acid binding protein II genes is coordinately regulated in human breast cancer cells. Oncogene. 2005; 24:4362–9. [PubMed: 15870697]
38. Li Q, et al. Identification and implantation stage-specific expression of an interferon-alpha-regulated gene in human and rat endometrium. Endocrinology. 2001; 142:2390–400. [PubMed: 11356686]
39. Thompson CJ, Tam NN, Joyce JM, Leav I, Ho SM. Gene expression profiling of testosterone and estradiol-17 beta-induced prostatic dysplasia in Noble rats and response to the antiestrogen ICI 182,780. Endocrinology. 2002; 143:2093–105. [PubMed: 12021174]
40. Mercier I, et al. Genetic ablation of caveolin-1 drives estrogen-hypersensitivity and the development of DCIS-like mammary lesions. Am J Pathol. 2009; 174:1172–90. [PubMed: 19342371]
41. Han X, et al. Role of estrogen receptor alpha and beta in preserving hippocampal function during aging. J Neurosci. 2013; 33:2671–83. [PubMed: 23392694]
42. Pedram A, Razandi M, Aitkenhead M, Hughes CC, Levin ER. Integration of the non-genomic and genomic actions of estrogen. Membrane-initiated signaling by steroid to transcription and cell biology. J Biol Chem. 2002; 277:50768–75. [PubMed: 12372818]

43. Levin ER. Bidirectional signaling between the estrogen receptor and the epidermal growth factor receptor. Mol Endocrinol. 2003; 17:309–17. [PubMed: 12554774]

44. Ding L, et al. Ligand-independent activation of estrogen receptor alpha by XBP-1. Nucleic Acids Res. 2003; 31:5266–74. [PubMed: 12954762]

45. Papa L, Germain D. Estrogen receptor mediates a distinct mitochondrial unfolded protein response. J Cell Sci. 2011; 124:1396–402. [PubMed: 21486948]

46. Haynes CM, Ron D. The mitochondrial UPR - protecting organelle protein homeostasis. J Cell Sci. 2010; 123:3849–55. [PubMed: 21048161]

47. Siegelin MD, et al. Exploiting the mitochondrial unfolded protein response for cancer therapy in mice and human cells. J Clin Invest. 2011; 121:1349–60. [PubMed: 21364280]

48. Kang BH, et al. Preclinical characterization of mitochondria-targeted small molecule hsp90 inhibitors, gamitrinibs, in advanced prostate cancer. Clin Cancer Res. 2010; 16:4779–88. [PubMed: 20876793]

49. Sin N, et al. Total synthesis of the potent proteasome inhibitor epoxomicin: a useful tool for understanding proteasome biology. Bioorg Med Chem Lett. 1999; 9:2283–8. [PubMed: 10465562]

50. Kramer A, Green J, Pollard J Jr, Tugendreich S. Causal analysis approaches in Ingenuity Pathway Analysis. Bioinformatics. 2014; 30:523–530. [PubMed: 24336805]

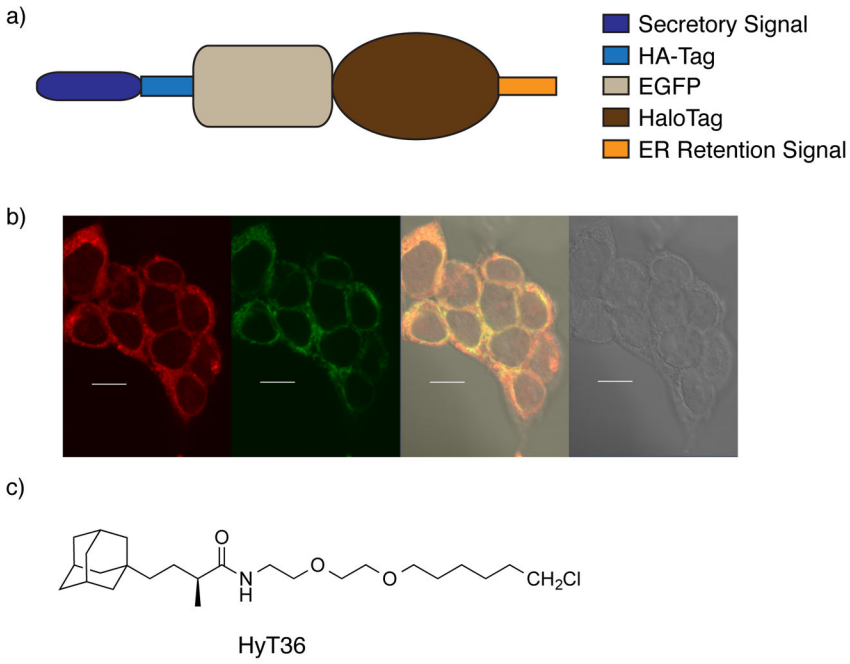

Figure 1.

The Endoplasmic Reticulum-localized HaloTag (ERHT) system. a) Schematic of ERHT construct. b) Confocal microscopy images showing an endoplasmic reticulum-staining dye (red), the ERHT protein (green), as well as a composite view including a differential interference contrast (DIC) image of the cells. Scale bar, 10μm c) Chemical structure of the small molecule, HyT36, used to destabilize the HaloTag protein.

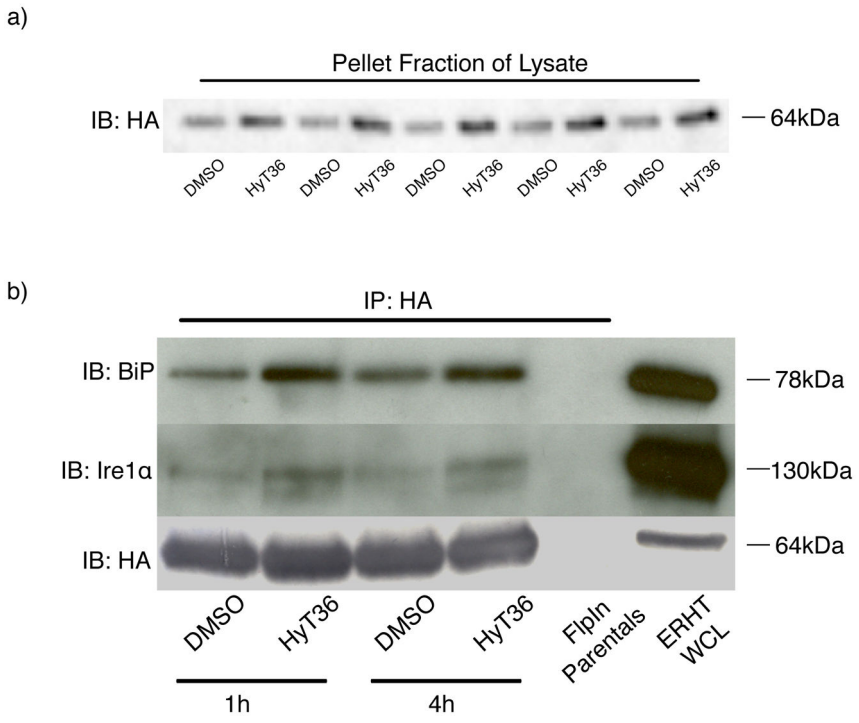

Figure 2.

HyT36 treatment causes destabilization of the ERHT protein. a) Immunoblot of the pellet fraction of ERHT cell lysate after treatment with DMSO or 10μM HyT36 b) Co-immunoprecipitation of BiP and Ire1α with the ERHT protein after a 1-hour or 4-hour treatment of cells with DMSO (0.1%) or HyT36 (10 μM). See Supplementary Fig. 16 for full gels.

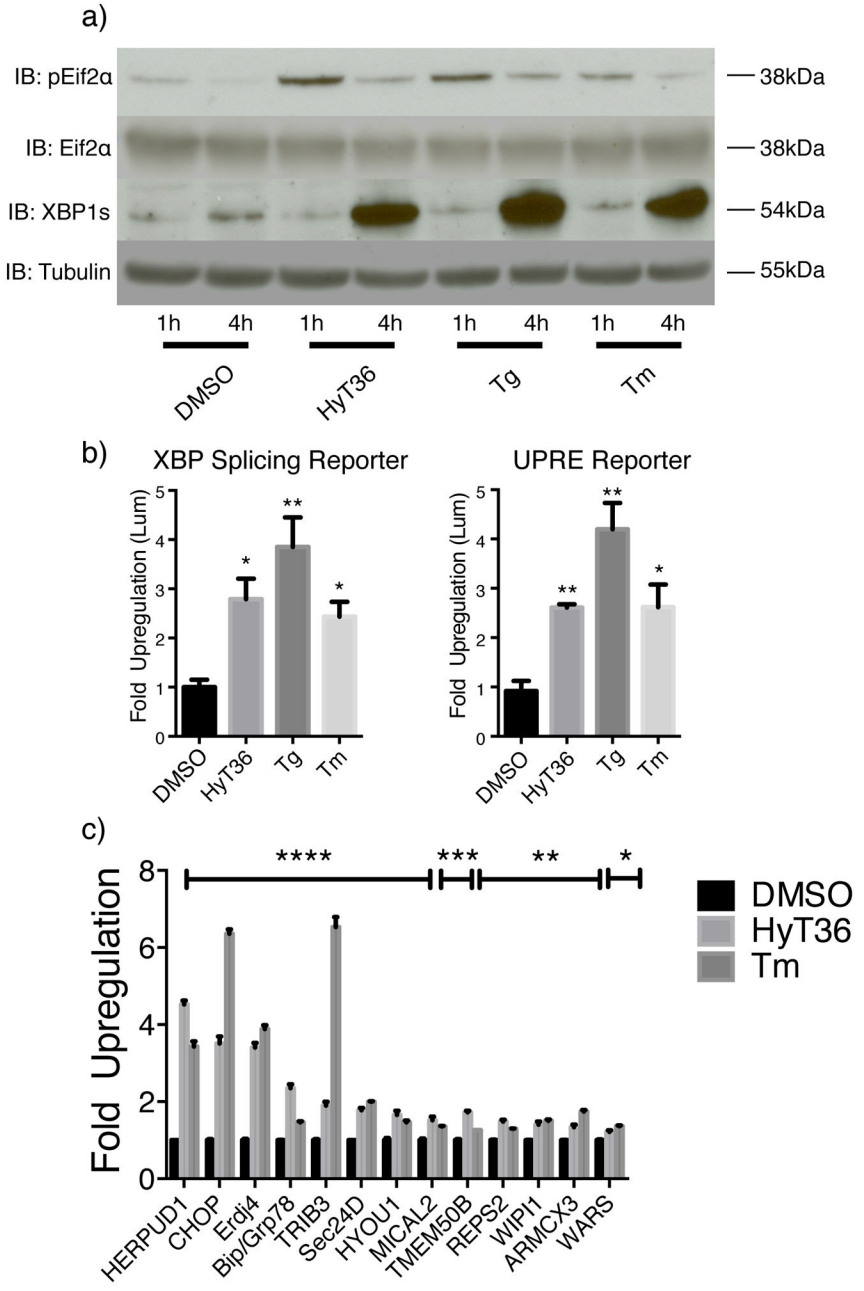

Figure 3.

HyT36 treatment of ERHT cells induces a UPR response comparable to tunicamycin and thapsigargin a) Western blot of ERHT cells after treatment with DMSO (0.1%), HyT36 (10 μM), thapsigargin (500 nM), or tunicamycin (5 μg/mL) for the indicated times. See Supplementary Fig. 17 for full gels. b) Luciferase reporter activity for Xbp1 splicing (left) and UPRE driven transcription (right) in ERHT cells. Treatments were with DMSO (0.1%), HyT36 (10 μM), thapsigargin (Tg, 500 nM), or tunicamycin (Tm, 5 μg/mL) for either 4 hours (XBP1 splicing reporter) or 12 hours (UPRE reporter). 20 wells of a 384-well plate were used for each treatment (n=20). c) Real-time quantitative PCR measurements of genes

upregulated in response to UPR activation. The data was collected in biological triplicates (n=3). All Data represents mean values ± SEM. (*: $p<0.05$; **: $p<0.01$; ***: $p<0.001$; ****: $p<0.0001$)

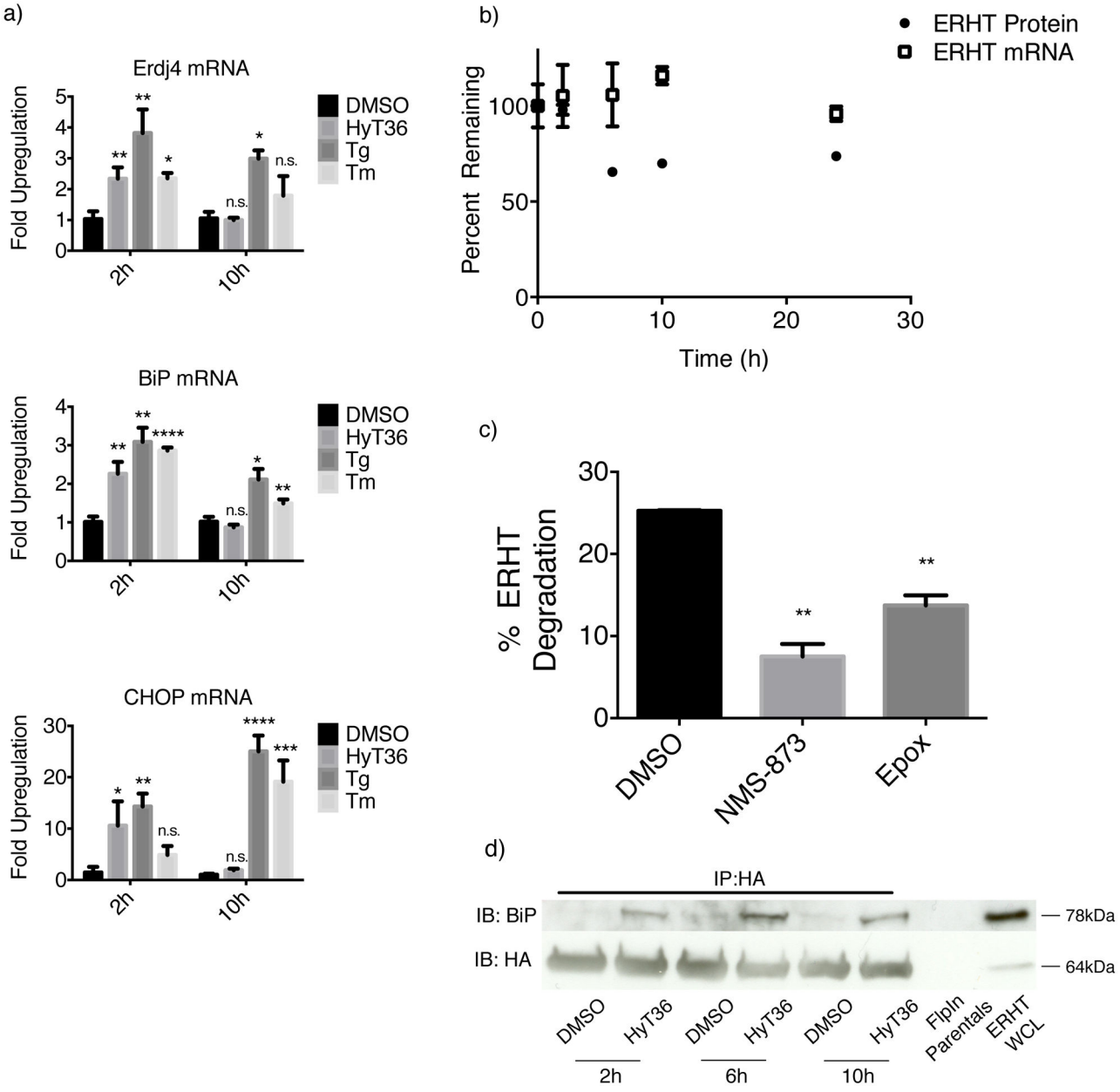

Figure 4.

Destabilization of the ERHT protein leads to acute ER stress. a) Real-time quantitative PCR analysis of UPR activation in ERHT cells after treatment with DMSO (0.1%), HyT36 (10 μM), thapsigargin (500 nM), or tunicamycin (5 μg/mL) for the indicated times. b) Normalized values for flow cytometry of GFP fluorescence (closed circles) to assess ERHT protein levels and qPCR (open squares) to assess ERHT mRNA levels after treatment with HyT36 (10 μM) for the indicated periods of time. c) The p97 inhibitor, NMS-873 (5μM), and the proteasome inhibitor, epoxomicin (100nM), prevent ERHT protein degradation induced by a 5.5h treatment with HyT36 (10 μM). d) Co-immunoprecipitation of BiP with the ERHT protein after a 2-hour, 6-hour, or 10-hour treatment with DMSO (0.1%) or HyT36

(10 μM). See Supplementary Fig. 18 for full gels. All data quantified herein was collected in biological triplicates (n=3) and represents mean values ± SEM. (n.s.: no significant difference; *: $p<0.05$; **: $p<0.01$; ***: $p<0.001$; ****: $p<0.0001$)

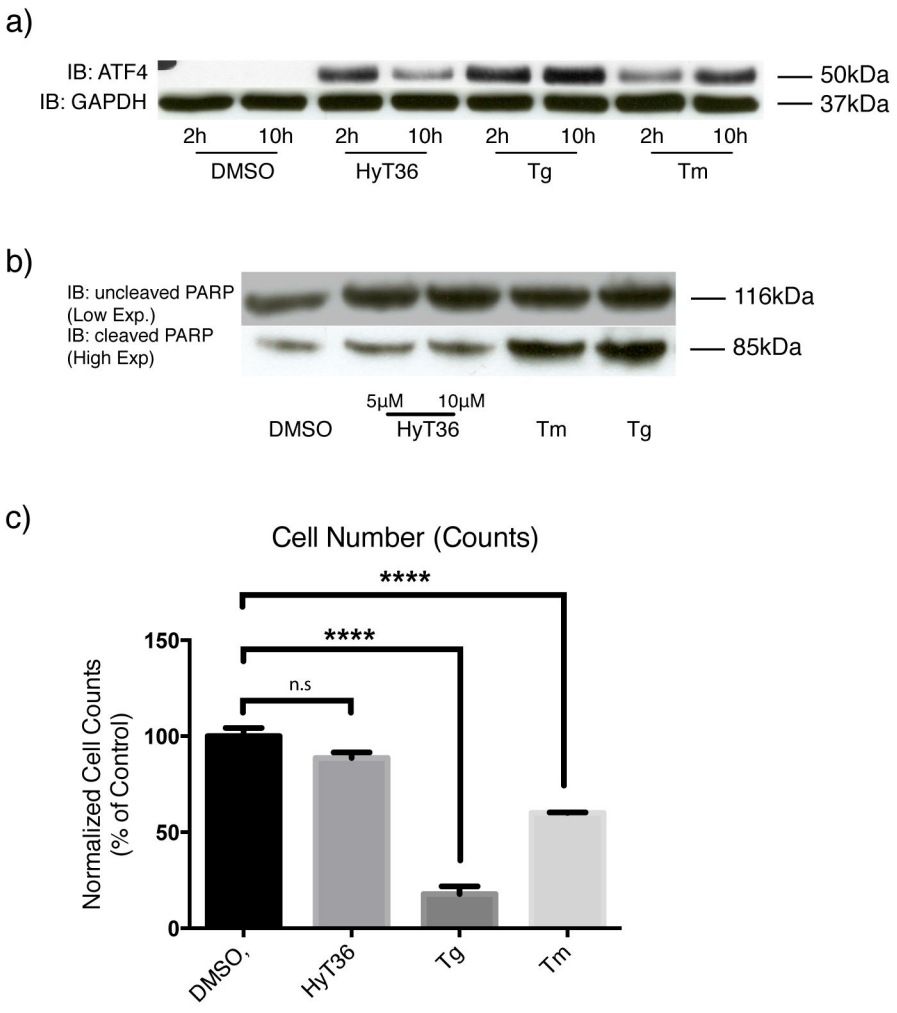

Figure 5.

The acute ER stress induced by HyT36 does not result in apoptosis. a) Western blot for ATF4 levels (PERK activity) after treatment with DMSO (0.1%), HyT36 (10 μM), thapsigargin (500 nM), or tunicamycin (5 μg/mL) for the indicated time periods. b) PARP cleavage, measured by Western blot, as a read-out of apoptosis after treatment with DMSO (0.1%), HyT36 (5 μM or 10 μM), thapsigargin (500 nM), or tunicamycin (5 μg/mL) for 24 hours. See Supplementary Fig. 19 for full gels. c) Cell counting to determine number of cells after treatment with DMSO (0.1%), HyT36 (10 μM), thapsigargin (500 nM), or tunicamycin (5 μg/mL) for 24 hours. The experiment was done in biological triplicates (n=3). Data represents mean values ± SEM. (n.s.: no significant difference; ****: $p<0.0001$)

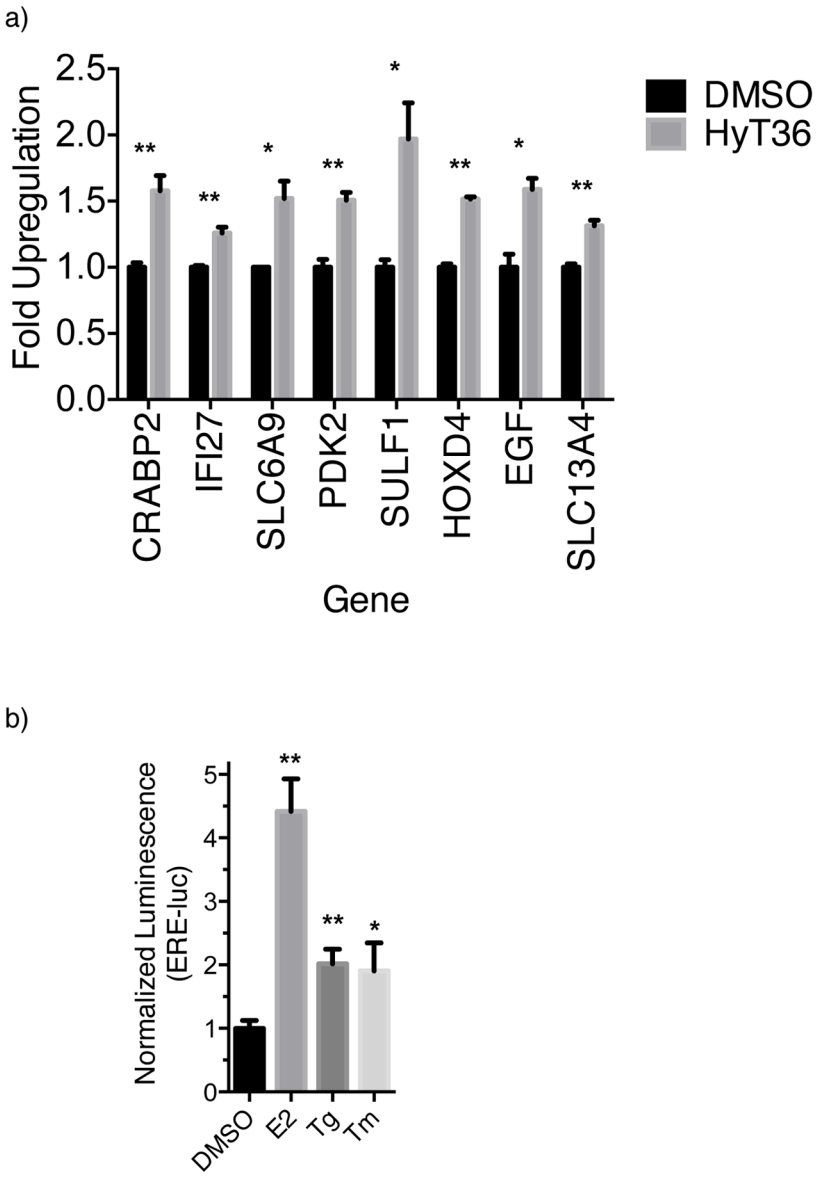

Figure 6.

Identification of estrogen signaling as a late-stage response to UPR activation. a) Real-time quantitative PCR of a subset of genes that were identified by Ingenuity Pathway Analysis as potentially regulated by ESR1 in the HyT36 10 hour sample, after a 10 hour treatment with DMSO (0.1%) or HyT36 (10 μM). The data was collected in biological triplicates (n=3) b) Estrogen response element (ERE) luciferase activity in MCF7 cells after a 24 hour treatment with DMSO (0.1%), estradiol (10 nM), thapsigargin (500 nM), or tunicamycin (5 μg/mL). 20 wells of a 384-well plate were used for each treatment (n=20). All data shown here represents mean values ± SEM. (*: $p<0.05$; **: $p<0.01$; ***: $p<0.001$; ****: $p<0.0001$)